

# A MONTE CARLO CALCULATION FOR NEUTRON RADIOGRAPHY FACILITY USING SEALED-TUBE NEUTRON GENERATOR

Jin-Hyoung Bai<sup>1</sup>, Myung-Won Shin<sup>2</sup>, Joo-Ho Whang<sup>1</sup>

<sup>1</sup>Department of Nuclear Engineering, Kyung Hee University, 1, Seocheon-dong, Giheung-gu, Yongin-si, Gyeonggi-do, 449-701, Rep. of Korea,

<sup>2</sup>SIRIUS Co., LTD., 3FL, 169-1, Juan-dong, Nam-gu, Incheon, 402-200, Rep. of Korea

## Abstract

Fast neutron radiography (FNR) is a promising non-destructive inspection technique that is especially suitable for non-destructive inspection of industrial products that are too thick or dense to be inspected by conventional thermal neutron radiography. In this study, shielding structures were designed and built within a limited space (that was part of an existing building) in order to protect both operators and nearby residents as well as the sensitive CCD-detection system. The scattering effects caused by the shields were assessed by the detector as well. A sealed-tube neutron generator was used as the neutron source. A Monte Carlo calculation was done using MCNP4C code which is capable of solving the coupling transport problem for neutrons and gamma rays. With the calculation, neutrons were emitted isotropically (14MeV) from a point-like source, and the history of the quantity was determined to discern a relative calculation error within 10%. The dose conversion factor (DCF) from ICRP74 was applied to convert the flux of neutrons and gamma rays. From the calculation results, the highest dose rate was 8.2mrem/week. However, due to the complexity of the shielding structures, there was a possibility that some noise could affect the imaging process. The performance and characteristics of each component was analyzed; the mirror, lens, scintillator and the cooled CCD camera. It was determined that the scattered neutrons together with the shielding structures were both able to cause some distortion within the detector system. For the future, we recommend that a Monte Carlo simulation be done to better determine the optical behaviour of scintillation detectors in order to improve detection efficiency.

## 1. Introduction

Fast neutron radiography (FNR) presents a promising nondestructive inspection technique due to the excellent penetration characteristics of fast neutrons. FNR is especially more suitable than conventional thermal neutron radiography when the inspection object is thick or dense.

An FNR inspection system consists of three major components: a neutron source, the inspection object and a neutron detector [1]. The quality of the radiographic image is affected by the results of each component. A fast neutron imaging detector system can consist of a scintillator, a mirror, an optical system, a charge-coupled device (CCD) camera and a shielding structure. For a real-time FNR system, a silicon intensifier target (SIT) tube camera was developed and tested [2]. The potential of a cooled CCD-detector system for these purposes depends on both its design and the inspection conditions, and has still to be investigated.

The aim of this study has been to investigate issues concerning the application of a cooled CCD-detector system for FNR using a sealed-tube neutron generator. A Sodern GENIE16C D-

T reaction-based neutron generator (made in France) was used as the neutron source for the fast neutron radiography. The maximum neutron generation rate of the GENIE16C is about  $2 \times 10^8$  n/sec and the neutron energy generated by the D-T reaction is 14MeV [3]. The difficulties of shielding are primarily caused by this high neutron energy. The shielding was designed to protect operators and passers-by in a limited space within the existing building. The scattering effect due to the shielding was assessed by the detector.

## 2. Selection and characterization of the CCD detector components

In this section, the validity of the cooled CCD camera was evaluated and the rationale for selecting the individual components described. In actuality, careful selection of the component mix and their fine-tuning may gain up to a few orders of magnitude of improved sensitivity.

A cooled CCD camera was developed [4] to serve as a neutron radiography detector. The basic principle of this detector is shown in Fig. 1. The neutron beam reaches the neutron converter screen after penetrating the sample. Because the CCD

chip can easily be damaged by neutron radiation, it is necessary to locate the camera outside the direct path of the neutron beam. Therefore, the light emitted from the converter screen is reflected onto the camera lens by a mirror and focused on the CCD chip by a lens. These components are located in a shielded housing together with shielding material to protect the cooled CCD camera from scattered neutrons and  $\gamma$ -rays.

The cooled CCD camera is connected to a PC to process and display the digitized image data.

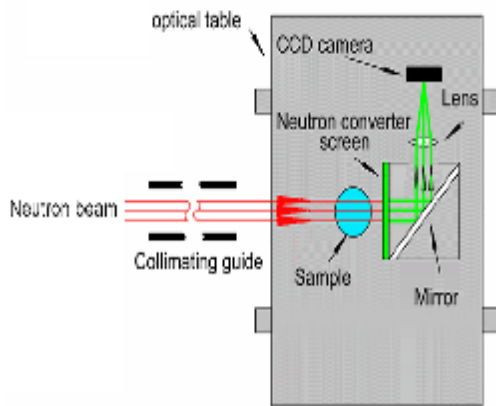


Figure 1: Schematic layout of fast neutron imaging.

### 2.1 Sensitive Fast Neutron Scintillator Screen

The NAG scintillator glass used in this study was manufactured by Applied Scintillation Technologies (UK) [5]. AST has developed and manufactures a variety of cerium activated lithium-free glass (NAG) scintillators for a wide range of applications. The NAG glass was specifically designed to be especially sensitive at detecting fast neutrons of 14MeV while having a low sensitivity to thermal neutrons and other radiations. Since the NAG is glass and opaque to its own light spectrum, the thickness of the glass is limited. This scintillator has its peak emission at 400nm. Detection efficiency with fast neutron energy is in the order of about 1%. Gamma sensitivity of the scintillator is between 30% and 50%. The after-glow effect as a source of distortion for the neutron radiographic image can be neglected for most applications.

### 2.2 Mirror and Lens

The scintillation light is deflected via an optical quartz mirror to the camera lens. An FNR system demands a high reflectivity of at least 90% of the light emitted by the NAG scintillator and should generate as low an amount of  $\gamma$ -rays as possible. Therefore, a 1~2 mm thick glass plate coated with Al and quartz as a protection layer was manufactured at the Korea Atomic Energy

Research Institute (KAERI). In order to obtain a higher reflectivity of over 95% for the blue region, silver should be used as it is more suitable than aluminium. Fig. 2 shows the mirror housing without the scintillator and mirror.

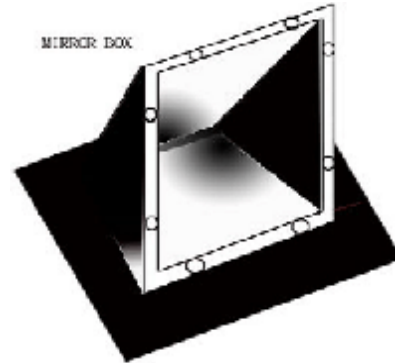


Figure 2: Mirror housing.

Because light transmission should be maximized and image distortion avoided, use of a high quality lens is extremely important. The desired image size is  $(26 \times 26) \mu\text{m}^2$ . The space available beside the facility is about 100cm. Decided by the design parameters, a standard high-quality 50mm Nikon F/1.2 lens was used. Our conclusion is that even high magnification systems should be installed in lenses with a low aperture setting and shorter focal length with the camera as close as possible to the scintillator screen. As most camera lenses require a minimum distance of 100cm for their built-in adjustable range to be effective, the system will require specially made mounting brackets with a thickness up to several millimetres to vary the width between the CCD-matrix and lens.

### 2.3 LN Cooled Digital CCD Camera

On a CCD chip, potential wells are formed below electrodes on the surface. Photo electrons are collected in these potential wells. On a classic CCD chip, the photons have to traverse the electrodes which usually consist of very thin aluminium layers. These electrodes are very transparent for blue light. On some CCDs, the sensitivity for 400nm drops down to 4% quantum efficiency, while others reach 16%. So-called back-illuminated CCDs are etched thin down to  $20\mu\text{m}$  and are illuminated from the back side where no coating exists. They reach up to more than 80% efficiency for blue light. The CCD chip produces a certain amount of thermal distortion, which ranges from several thousand electrons per second at room temperature down to less than one electron per hour at  $-120^\circ\text{C}$  for a Roper Scientific liquid-nitrogen cooled CCD camera.

The pixel array of the high-precision CCD chip in this camera is 1340×1300 with a pixel size of (26.8×26)μm<sup>2</sup> and provides 16-bit digitization (65,535 gray levels). The quantum efficiency of the LN cooled CCD camera is in the range of 84~94% for wavelengths from 350nm to 800nm. Figure 3 shows the LN cooled CCD camera.



Figure 3: Image of the Liquid-Nitrogen cooled CCD camera.

For application at a sealed-tube neutron generator, high-speed exposures are necessary if the spectral information coded in the pulse duration is to be used. Scintillation of the NAG glass typically decays to 10% in 1ms without an after-glow. The decay time of the Bicron BC-720 fast neutron detector is 0.2 μs.

A major problem with all images taken with a CCD camera is the background gamma rays that hit the CCD chip itself. Therefore, it is imperative that the CCD chip be properly shielded. The detection efficiency for gamma rays is low, but detected gammas form a local electron cascade which will cause a local overflow of the CCD chip and produce white spots in the image.

### 3. Shielding calculation

The shielding calculation was done using MCNP4C code which is capable of solving the coupling transport problem for stray neutrons and gamma rays. Upon calculation, a neutron source having an isotropy of 14MeV was delineated, and the history of the quantity was determined to maintain a relative calculation error within 10%. The dose conversion factor (DCF) from ICRP74 was applied to convert the flux of neutrons and gamma rays.

In the fast neutron stream generated by the D-T reaction, there were difficulties encountered such that neutron absorbing material could not be used for shielding differently from the case of thermal neutrons. Therefore, it almost depends upon energy

slowing down due to collision with shielding material. In a previous study, TiH<sub>2</sub> and ZrH<sub>2</sub> were evaluated for use as fast neutron shielding [6]. However, since these materials are expensive and can not be commercially obtained, the shielding structure was designed using concrete and general polyethylene (PE). SUS304 was used for the structural components. The shielding was designed with the following parameters.

- ① Operation time was expected to be less than 40 hours/week with the limited dose rate value recommended by the Ministry of Science & Technology (MOST) of 10.0 mrem/week.
- ② Both the irradiation and operation rooms were constructed within a limited space ((5.5m(W) x 7.5 m(D) x 3.2 m(H)). The irradiation room was designed to maintain over 4.0m to depth according to Korean Standards.
- ③ Sinking of the floor had to be considered to determine the thickness of the shielding wall.

### 3.1 Results of the Shielding calculation

Figures 4 and 5 show the shielding structure. The thickness of the concrete shielding wall was determined to be 60cm according to restrictions 2 & 3. Because this concrete wall could not satisfy the limiting dose rate value, an additional shield made of PE was deemed necessary. The PE thickness on the side was 30.0~35.0cm, and the one on top was 55.0cm.

The thickness of the concrete ceiling was 12.0 cm, so shielding there was very weak. For that reason a 22.0cm thick PE layer was added to the entire ceiling of the irradiation room.

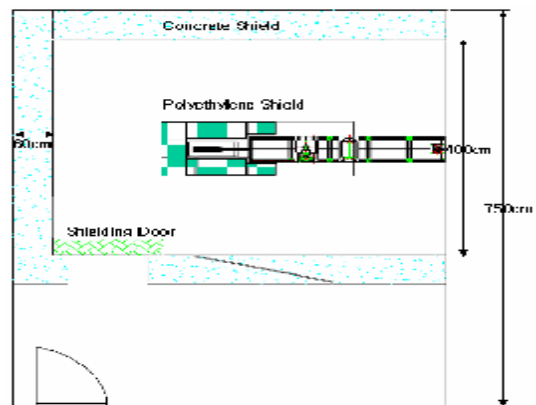


Figure 4: Plan view of the shielding structure including the exposure room and operation room.

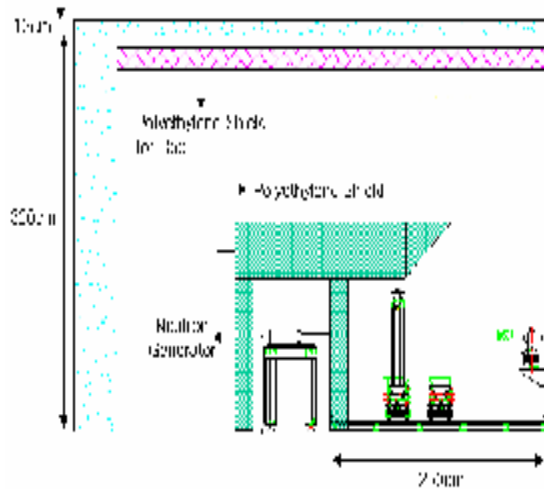


Figure 5: Side view of shielding structure for the irradiation room.

Assessment of the dose rate was conducted by finely dividing the face of the exterior wall of the shield into a node of 10cm x 10cm size. In Figure 6, the dose rate distribution assessed at the wall face of the operation room is shown. A maximum value of 0.205 mrem/hr was exhibited at the shielding door of which the thickness of the shield was relatively thin. This indicates that the limit value was not exceeded despite considering a maximum value of 95% confidence.

Also, maximum values assessed at the walls facing the other directions exhibited much lower values than the limit value, respectively 0.137 mrem/hr, 0.145 rem/hr and 0.168 mrem/hr.

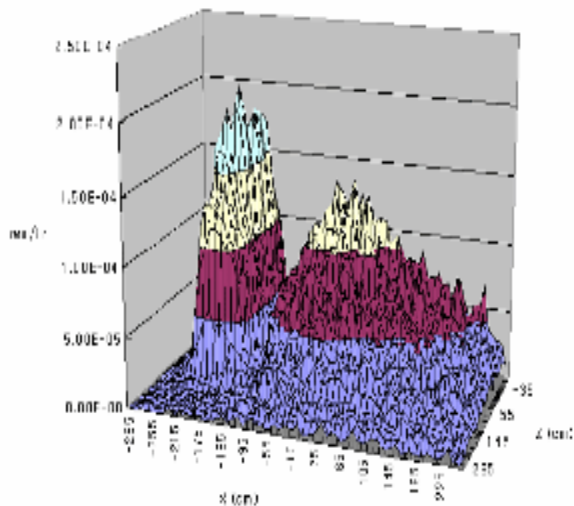


Figure 6: Dose rate distribution at the shielding wall surface of the operation room.

### 3.2 Analysis of scattering effects at the detector due to the shielding structure

Since the dose rate could not be satisfied only with the concrete shielding wall due to the insufficient space available, a method for further shielding it with a PE layer was devised. Nevertheless, scattered neutrons were still able to cause distortion in the detector system. The following four cases were evaluated for neutron scattering effects with the distance between the neutron source and object assumed to be 1.0m.

- ① Model 1 : all shielding structures were considered,
- ② Model 2 : only concrete wall was considered,
- ③ Model 3 : no shielding structure, and
- ④ Model 4 : detector is covered with PE shield (10cm size).

In Table 1 and Figure 7, the ratio of incident neutrons without scattering to all incident neutrons for each of the 4 cases was compared at the detector location. It was determined that as the shielding structure becomes more complicated, more distortion may occur due to the increased scattering of neutrons. In the scattered neutron energy spectrum, most of the neutrons were distributed near 0.1 MeV. This means that use of a neutron absorbing material is not effective for shielding this system.

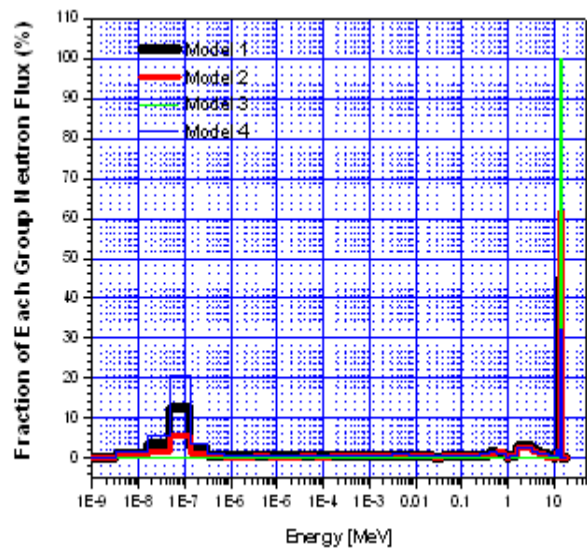


Figure 7: Fraction of each group neutron flux as the shielding structure

*Table 1: Ratio of incident neutrons without scattering with shielding structures*

|         | Neutrons without scattering /<br>all of incident neutrons<br>(at detector location) |
|---------|-------------------------------------------------------------------------------------|
| Model 1 | 46.00 %                                                                             |
| Model 2 | 62.00 %                                                                             |
| Model 3 | 100.0 %                                                                             |
| Model 4 | 32.00 %                                                                             |

Although the distortion caused by scattering effects could be partly reduced by more precise positioning of the system components, this is not really an effective course to pursue [7]. Increasing the reaction rate of the detector material with fast neutrons (14MeV) without scattering, and decreasing the scattered neutron flux at the detector location are more effective methods. Therefore, proper selection of detector materials and the overall design of the collimator are very important.

#### 4. Conclusion

The aim of this study was to study issues concerned with the application of a cooled CCD-detector system for an FNR system using a sealed-tube neutron generator. In the case of a sealed-tube neutron generator, the point-like source emits neutrons isotropically. However, this condition increases additional background radiation. A proper shielding structure for the detector is needed to eliminate background radiation and CCD chip damage. Another problem is caused by the scintillator which has a very low detection efficiency of only 1~2% for fast neutrons. For the future, we recommend further study using a Monte Carlo simulation for the optical behavior of scintillation detectors in fast neutron imaging to improve detection efficiency.

The shielding was designed conservatively to cope with the conditions that the GENIE16C would be operated at maximum power during operating time and occupancy would be 100%. From the calculation results, the highest dose rate was 8.2mrem/week, which did not exceed the acceptable safety limit. Therefore, it can be said that the proposed shielding adequately protected both operators and passer-bys. However, because the shielding structure caused some distortion to the imaging process, further R&D is needed to

better design the collimator and develop more effective detector material.

#### 5. Acknowledgment

This calculational work was financially supported by the SRC/ERC program of MOST/KOSEF and parts of the facility was financially supported by MOCIE through IERC program.

#### 6. References

- [1] J.C. Domanus, *Practical Neutron Radiography*, Kluwer Academic Publishers, Dordrecht, 1992.
- [2] M. Matsubayashi et. al., Proc. 6<sup>th</sup> World Conf. on Neutron Radiography, 17-21 May 1999.
- [3] E. Jolly, *GENIE16-Instruction for Use*, SODERN ref 4011-143-6934-0F, 2001.
- [4] H. Pleinert, E. Lehmann, S. Korner, Design of a New CCD-Camera Neutron Radiography Detector, *Nuclear Instruments and Methods A* 399, pp 382-390, 1997.
- [5] Applied Scintillation Technologies data sheet # 42 on <http://www.appsintech.com>.
- [6] Choonsik Lee, et. al., A Preliminary Study on Neutron Shielding for High Energy Neutron Generator, *Proceeding of KNS Fall Meeting*, October 30-31, 2003.
- [7] S.Cluzeau, Some Aspects of Neutron Radiography when Using a Low Output Neutron Source, *Fifth Meeting of the European Neutron Radiography Working Group*, June 25-27, 1997.